

# Development towards a nested hydrodynamic model for the numerical analysis of ocean wave energy systems

Jost Kemper, Christian Windt, Kai Graf and John V. Ringwood

**Abstract**—Numerical wave tanks (NWTs) provide a cost efficient and accurate tool to assess the complex fluid dynamic field around wave energy converters (WECs). In recent years, high fidelity methods based on the Reynolds-averaged Navier-Stokes (RANS) equations are increasingly applied for this type of analysis. However, the computational cost for a RANS-based analysis of WECs is very high, compared to lower fidelity models based on e.g. potential flow (PF) theory. Nested hydrodynamic models can combine the advantages of RANS and PF solvers. Only the near flow field of the WEC is considered in the RANS solver, whereas the far field is solved using the PF model. Thus, the overall computational effort can be decreased, with respect to pure RANS models, while maintaining a high accuracy of the solution in the region local to the device. This paper presents the development towards a new, two-way coupled, nested hydrodynamic model for future application in wave energy. The proposed nested model is successfully verified and validated against theoretical and experimental data. Some limitations are found, which hamper the applicability of the method with respect to parallelised and three dimensional cases, and should be addressed as part of future work.

**Index Terms**—Wave energy, Computational fluid dynamics, Numerical wave tanks, Domain decomposition

## I. INTRODUCTION

**H**YDRODYNAMIC analysis in numerical wave tanks (NWTs) plays an important role in the design and optimisation of wave energy converters (WECs). Numerical models are widely applied to fluid flow problems in engineering. Yet, studies of WECs in power production mode, i.e., resonant motion with the incident wave field and subject to control action, pose a number of challenges to any numerical modelling approach, which can be summarised as:

- Wave generation and absorption
- Wave propagation
- Wave-structure interaction
- Large amplitude body motion

With the increased availability and decreased cost of computational resources, computational fluid dynamics (CFD) methods, based on the Reynolds-averaged Navier-Stokes (RANS)

equations, are increasingly applied for NWT experiments in recent years [1]. CFD-based numerical wave tanks (CNWTs) are capable of accurately modelling the relevant hydrodynamic effects, such as viscous boundary layers, turbulent and separated flow. However, their computational cost is very high and may become prohibitive, when large scale wave propagation effects have to be considered, e.g. in the case of WEC arrays. Thus, the application of CNWTs is often limited to specific research questions and, usually, single WEC devices.

In contrast to RANS-based CNWTs, potential flow (PF) based methods are widely used in industry and academia [2]. The assumption of inviscid and irrotational flow significantly reduces the computational cost for these NWTs. However, while the pure wave propagation problem is usually well described by PF theory, it is understood that the employed linearisations do not hold for the complex flow in the near field of WECs. In particular when device motion is amplified through control action, it has been shown that the use of PF-based NWTs decreases the accuracy of the results [3].

Thus, there is a demand for a numerical model which combines high accuracy with moderate computational requirements, for power production assessment of WECs. Nested models are developed to achieve these properties, by connecting different flow solvers, based on the computational requirements and possible linearisation in different spatial areas of the flow field. In naval science, the strategy of coupling RANS and PF solvers to obtain high fidelity for viscous effects and fluid structure interaction, while profiting from the computational efficiency of PF solution for less complex parts of the problem, is well known [4] [5] [6]. For these nested RANS-PF models, the computational domains are usually arranged as depicted in Fig. 1. Here, the small RANS domain, which often represents the near field of a structure, is surrounded by a larger PF domain, for wave generation, propagation and absorption.

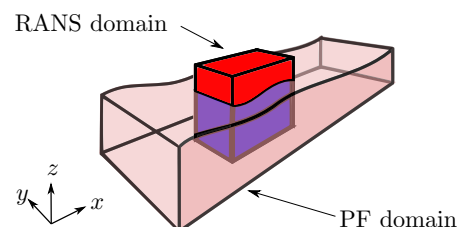


Fig. 1. Typical domain setup for nested models

Paper ID: 1414, Conference track: Wave hydrodynamic modelling

J. Kemper and K. Graf are with the Department of Naval Architecture and Maritime Technology, Faculty of Mechanical Engineering, University of Applied Sciences Kiel, Grenzstraße 3, 24105 Kiel, Germany (e-mail: jost-kemper@gmx.de; kai.graf@fh-kiel.de)

C. Windt and J. V. Ringwood are with the Department of Electronic Engineering, Centre for Ocean Energy Research, Maynooth University, Maynooth, Co. Kildare, Ireland (e-mail: christian.windt.2017@mumail.ie; john.ringwood@mu.ie)

Two different types of nested models can be distinguished, depending on how the coupling between the different flow solvers is achieved. These are:

- one-way coupled models
- two-way coupled models

One-way coupled models only transfer solution information between the coupled solvers in a single direction. Consequently not all the solution information can be shared between the solvers. Thus, wave propagation between the models is also limited to one direction.

A simple one-way coupled method was described by Lachaume *et al.* [7]. Here, breaking of solitary waves on a sloping beach was studied using a coupled boundary element method (BEM)-RANS approach. This model was extended for three-dimensional simulation of breaking waves in [8].

Another one-way coupled model was presented by Paulsen *et al.* [12]. This model couples the fully non-linear potential flow (FNLPF) solver OceanWave3D [11] to the RANS wave generation and absorption toolbox waves2Foam [13], in the OpenFOAM environment. Paulsen *et al.* find that this model has the potential to improve computationally efficient studies of realistic extreme wave impact on monopiles.

Two-way coupled models exchange solution information bidirectionally between both solvers. This way, wave propagation between the models is possible in both directions.

A two-way coupled model is described by Kim *et al.* [9], where a BEM and RANS model are coupled in a two-way fashion, using relaxation zones between the domains of both models. Kim *et al.* conclude that their model significantly reduces the computational demand for high fidelity simulation of random waves.

A more straightforward approach to a two-way coupling has recently been presented by Verbrugge *et al.* [10]. In this study, the FNLPF solver OceanWave3D [11] is coupled to a smoothed particle hydrodynamics (SPH) model for studying wave interaction with floating bodies. It is found that the model significantly reduces the SPH domain size and, thus, the computational effort.

Within the course of the present paper, several studies were carried out with the model presented by Paulsen *et al.* [12]. From these studies, the potential of the nested approach was clearly seen. However, the distinct disadvantages of the implemented one-way coupling also became evident. Since, for a one-way coupling, the PF wave field remains unaffected by the wave-structure interaction in the RANS domain, two problems arise:

- Large scale interaction phenomena between WECs, located in several small RANS domains inside the PF domain, cannot be studied.
- Wave reflection from the boundaries of the RANS domain may become problematic, since a misfit between the RANS wave field and the unbiased PF solution is present at these boundaries.

It was thus concluded that a two-way coupled model is needed for an efficient wave energy NWT, with the ability of studying large scale WEC interaction. In this paper, a concept for a two-way coupled nested hydrodynamic model is presented. The

development is based on the one-way coupling by Paulsen *et al.* [12], from which part of the source code is taken. The applied two-way coupling methodology is inspired by Verbrugge *et al.* [10].

The remainder of this paper is organised as follows. First, in Section II, an overview is given of the FNLPF and RANS modelling approaches. The coupling concept by Paulsen *et al.* [12] is presented in Section III, together with the proposed two-way coupling approach. Verification and validation studies for the new model are presented in Section IV. A case study to show its potential for wave energy applications is presented in Section V. Some limitations of the proposed model are discussed in Section VI. Finally, conclusions are drawn in Section VII and future work is presented in Section VIII.

## II. HYDRODYNAMIC MODELLING

### A. RANS solver

With the *interFoam* solver, the OpenFOAM framework features a RANS free surface flow solver, based on the Volume of Fluid (VOF) free surface modelling technique [14]. *interFoam* forms the basis of the wave generation and absorption toolbox waves2Foam [13], which is used in this paper. A brief overview of the theory behind *interFoam* will be given in this section. For a more detailed description of the theory, the interested reader is referred to [15].

For a combined flow of incompressible water and air, the conservation equations for momentum and mass, in an Eulerian reference frame, can be expressed as

$$\frac{\partial \rho \mathbf{u}}{\partial t} + \nabla \cdot (\rho \mathbf{u} \mathbf{u}) = -\nabla p + \rho \mathbf{g} + \nabla \cdot \mu_e (\nabla \mathbf{u} + (\nabla \mathbf{u})^T) \quad (1)$$

and

$$\nabla \cdot \mathbf{u} = 0, \quad (2)$$

respectively. In (1) and (2),  $\mathbf{u}$  is the velocity field,  $p$  is the pressure and  $\rho$ ,  $\mathbf{g}$  and  $\mu_e$  are fluid density, gravitational acceleration and effective dynamic viscosity, respectively. The latter is obtained by turbulence closure models.

Local values for  $\rho$  and  $\mu_e$  of the fluid mixture depend on the local water volume fraction  $\alpha$  as follows:

$$\rho = \alpha \rho_{water} + (1 - \alpha) \rho_{air} \quad (3)$$

$$\mu_e = \alpha \mu_{water} + (1 - \alpha) \mu_{air}. \quad (4)$$

$\alpha$  is subject to the conservation equation

$$\frac{\partial \alpha}{\partial t} + \nabla \cdot \mathbf{u} \alpha + \nabla \cdot \mathbf{u}_r \alpha (1 - \alpha) = 0. \quad (5)$$

In (5), the last term on the left hand side is a compression term, which is introduced to avoid smearing of the fluid interface, with  $\mathbf{u}_r$  being a relative velocity, pointing in a direction perpendicular to the free water surface [16]. A bounded solution of (5) is obtained by *interFoam*, using the multi-dimensional limiter for explicit solution (MULES) scheme, which is described in [16]. The pressure velocity coupling is solved using the pressure-implicit with splitting of operators (PISO) algorithm [17].

1) *Wave generation and absorption*: The waves2Foam toolbox provides inlet and outlet boundary conditions for wave generation and absorption in OpenFOAM. The fluid velocity  $\mathbf{u}$  and the water volume fraction  $\alpha$  are prescribed as Dirichlet type boundary conditions, where the values are derived from wave theories, such as Stokes first, second and fifth order, stream function or cnoidal theory. No theory is available for the pressure at the boundary. Therefore, waves2Foam uses a Neumann-type boundary condition for the pressure, which is physically incorrect, as stated in [18], and causes the wave to collapse. To avoid this, relaxation zones have to be installed at the boundaries, which also serve the purpose of avoiding wave reflection from the boundaries. Inside the relaxation zones, the solution  $\theta$  of the variables  $\mathbf{u}$  and  $\alpha$  is given by

$$\theta = \gamma \theta_{\text{computed}} + (1 - \gamma) \theta_{\text{target}}, \quad (6)$$

where  $\gamma$  is the relaxation weight, which varies smoothly between 0, at the boundary, and 1, at the interface to the free fluid domain, following

$$\gamma(x_R) = 1 - \frac{\exp(x_R^{3.5}) - 1}{\exp(1) - 1} \quad \text{with} \quad x_R \in [0; 1]. \quad (7)$$

This method ensures that the target solution is maintained, while a physical pressure solution is developed inside the fluid domain.

### B. FNLPF solver

The FNLPF solver OceanWave3D was presented in 2009 by Ensing-Karup *et al.* [11], as a “tool suitable for large scale simulation of nonlinear wave-wave, wave-bottom and wave-structure interaction in the coastal and offshore environment” [11, p. 2100]. Unlike many potential flow solvers, OceanWave3D calculates the full three-dimensional flow field, by directly solving the Laplace equation. At the same time, OceanWave3D avoids the limited applicability of Boussinesq-type potential flow models, by implementing the full nonlinear free surface boundary conditions. An overview of the theoretical basis of the method will be given here, while a complete description of the theory and solution techniques for OceanWave3D can be found in [11] and [19].

A Cartesian coordinate system is defined with its origin on the still water plane and the  $z$ -axis normal to this plane, pointing upwards. Irrotational flow of an incompressible, inviscid fluid is assumed, for which the problem of non-breaking free surface waves can be described in terms of the velocity potential,  $\phi$ , and the  $z$ -position of the free water surface,  $\eta$ . Considering only the free surface values of  $\phi$ , the kinematic free surface boundary condition can be expressed in terms of the potential function of the horizontal free surface velocities  $\tilde{\phi}$ , the vertical free surface velocity  $\tilde{w}$ , and  $\eta$ , as follows

$$\frac{\partial \eta}{\partial t} = -\nabla \eta \cdot \nabla \tilde{\phi} + \tilde{w}(1 + \nabla \eta \cdot \nabla \eta). \quad (8)$$

Equation (8) states that a fluid particle, located at the free surface, must always remain on the free surface.

In the same way, the dynamic free surface boundary condition may be obtained by rewriting the Bernoulli equation for

an unsteady fluid, and setting the pressure at the free surface ( $z = \eta$ ) to 0. It reads

$$\frac{\partial \tilde{\phi}}{\partial t} = -g\eta - \frac{1}{2} \nabla \tilde{\phi} \cdot \nabla \tilde{\phi} + \frac{1}{2} \tilde{w}^2 (1 + \nabla \eta \cdot \nabla \eta). \quad (9)$$

In (8) and (9),  $\nabla = [\partial/\partial x, \partial/\partial y]$  is the gradient operator, which is defined in the horizontal plane only. Equations (8) and (9) can be used to integrate the problem forward in time. In OceanWave3D, this is achieved using a fourth-order Runge-Kutta scheme. However, a closed solution of (8) and (9) does not exist, since the vertical velocity at the free surface must be known. Consequently, the problem has to be closed by solving the Laplace equation for the fully three-dimensional velocity potential  $\phi$ , along with the kinematic bottom boundary condition:

$$\nabla^2 \phi + \frac{\partial^2 \phi}{\partial z^2} = 0, \quad -h \leq z < \eta \quad (10)$$

$$\frac{\partial \phi}{\partial z} + \nabla h \cdot \nabla \phi = 0, \quad z = -h. \quad (11)$$

In (11),  $h$  is the variable water depth below the still water level ( $z = 0$ ). On the vertical boundaries of the domain, homogeneous Neumann boundary conditions are applied.

OceanWave3D solves the Laplace problem using a flexible order finite difference scheme [11]. Wave generation and absorption is realised using a relaxation zone approach, as presented by Larsen and Dancy [20]. Wave theories are implemented for the generation of regular and irregular waves. In addition, inhomogeneous time varying Neumann boundary conditions for  $\phi$  can be applied to replicate a wave maker paddle signal from physical experiments [21].

## III. NESTED HYDRODYNAMIC MODEL

The present paper aims to develop a new nested hydrodynamic model, by coupling the solvers detailed in Section II in a two-way fashion. This section will explain the coupling concept, which establishes the desired information transfer. Before this, a more detailed overview will be given of the one-way coupled method by Paulsen *et al.* [12].

### C. One-way coupling

As mentioned in Section I, the method of Paulsen *et al.* [12] couples the FNLPF solver OceanWave3D [11], to the RANS wave generation and absorption toolbox waves2Foam [13], in the OpenFOAM environment. The method represents a one-way coupling and is implemented as a “numerical wave theory” for waves2Foam. The benefit of the method is that large scale wave propagation over an arbitrary bathymetry can be studied in OceanWave3D, and thus a fully developed wave field can be provided to waves2Foam.

Since OceanWave3D solves for the full three-dimensional flow field, the fluid velocities and surface elevation can be interpolated for any arbitrary position in the domain. This includes the area occupied by the OpenFOAM domain (see Fig. 1). Dirichlet-type boundary conditions for velocity and water volume fraction can thus be defined for all boundary faces of the OpenFOAM domain on the basis of the known FNLPF solution, as explained in Section II-A1. The relaxation

zones, used by waves2Foam to establish the wave field in the OpenFOAM domain, also use the OceanWave3D solution as target value (see (6)).

At each time step, first the FNLPF problem is solved by OceanWave3D, then the solution at the boundaries and inside the relaxation zones of the OpenFOAM domain is evaluated, and the OpenFOAM boundary conditions are formulated accordingly, before the RANS problem is solved by OpenFOAM, using the same time step size.

#### D. Two-way coupling

The aim of the present work is to overcome the disadvantages of one-way coupling, which were described in Section I, by transferring the OpenFOAM solution back to OceanWave3D, and thus establish a two-way coupling between the solvers. This opens the possibility of studying large scale interaction effects of multiple structures, which may be placed in several OpenFOAM domains, and also avoids a misfit of the solutions at the boundaries, which may lead to artificial wave reflection, as pointed out in Section I. In the following, first the general organisation of the coupled solution process will be explained, before the reconstruction of the FNLPF velocity potential on the basis of the RANS velocities is further detailed. Finally, a discussion of the proposed approach is presented, and some adjustments to the initial coupling methodology are introduced.

1) *Time stepping approach:* For a two-way coupling, the two solvers are required to run simultaneously, exchanging information at each time step. The temporal organisation of the different solution steps represents a challenge for any two-way coupled method. One solver has to be run first, i.e. without any information from the other solver, for the current time step. When the information transfer is established through boundary conditions, which both solvers provide to each other, as in [9], a situation arises, where one of the solvers has to perform the same time step twice. Once, to be able provide boundary conditions to the other solver, and again using the boundary conditions obtained from the other solver. To avoid the dual solution of the same time step, in the proposed coupling, the solution information is transferred as follows:

- 1) First the FNLPF problem is solved by OceanWave3D in the entire domain, including the area occupied by the OpenFOAM domain.
- 2) OceanWave3D is now able to provide boundary conditions for the RANS problem, as in the one-way coupled case (see Section III-C).
- 3) Then, the RANS problem is solved by OpenFOAM in a significantly smaller domain, compared to the OceanWave3D domain, using the same time step size.
- 4) Finally, the RANS solution for the free surface quantities  $\tilde{\phi}$ ,  $\eta$  and  $\tilde{w}$  are imposed onto the FNLPF solution in the area occupied by the OpenFOAM domain.

By this procedure, a RANS corrected version of the free surface position and velocities is obtained. The time integration of the FNLPF problem can then continue on the basis of the corrected quantities. The procedure is also depicted in Fig. 2.

It should be noted that, in OceanWave3D, only the free surface quantities can be corrected in this manner, since any correction to the internal flow field would not have an influence on the solution of the Laplace problem for the next time step.

2) *Reconstruction of the velocity potential:* As stated in Section III-D1 the FNLPF free surface velocity potential  $\tilde{\phi}$  (amongst others) is corrected during the two-way coupling procedure, based on the RANS solution. However,  $\tilde{\phi}$  does not exist in the RANS solution. Therefore, the velocity potential has to be reconstructed on the basis of the RANS velocities at the free surface. To achieve this, several methods were tested. Finally, an approach, considering a first order temporal integration of  $\tilde{\phi}$ , was chosen. Using (9), along with the solution of the previous time step  $\tilde{\phi}_{t-1}$ , and the corresponding discrete temporal derivative  $\Delta_{\tilde{\phi}_{t-1}}$  (as obtained by the solution of (9)), the solution for the current time step  $\tilde{\phi}_t$  can be calculated as

$$\tilde{\phi}_t = \tilde{\phi}_{t-1} + \Delta_t \frac{\Delta_{\tilde{\phi}_t} + \Delta_{\tilde{\phi}_{t-1}}}{2}, \quad (12)$$

where  $\Delta_t$  is the size of the last time step. Despite its simplicity, this approach yielded satisfactory results in all tests, and seemed more robust than a spatial integration, which was also tested.

3) *Discussion of the approach and adjustments:* The approach of probing velocities right at the free water surface in OpenFOAM, and interpreting them as equivalent to the velocities represented by the FNLPF free surface velocity potential  $\tilde{\phi}$ , may be questionable, since unphysical velocities in the interface region are a well known problem of the VOF free surface modelling technique [22]. In fact, during preliminary tests, an air circulation built up in the OpenFOAM domain, which lead to a gradual increase in the horizontal free surface velocity over time. These unphysical horizontal velocities were coupled to OceanWave3D, eventually causing the solution process to diverge.

Since any attempt to filter out the unphysical velocities, or extrapolate the free surface velocity from values along the water column, would have created a further source of uncertainty, it was decided not to couple the horizontal free surface velocities from OpenFOAM to OceanWave3D. The coupling was thus restricted to the surface elevation  $\eta$  and the vertical free surface velocity  $\tilde{w}$ , which produced satisfactory results.

#### IV. VERIFICATION AND VALIDATION

The developed two-way coupling approach has to be verified and validated carefully, to ensure its accuracy and stability.

The spatial and temporal discretisation, for all cases presented in this section, is based on convergence studies. Sufficient convergence was determined based on the mean wave height, using convergence measures described in [23]. The studies indicate that, for the OpenFOAM domain, a spatial discretisation of 15 cells per wave height (CPH) and 150 cells per wave length (CPL) is sufficient for the cases considered. However, for the simpler verification cases, where no dedicated convergence studies were carried out, 20 CPH is chosen. The CPL value is usually predetermined by the CPH value and the maximum cell aspect ratio, which is between

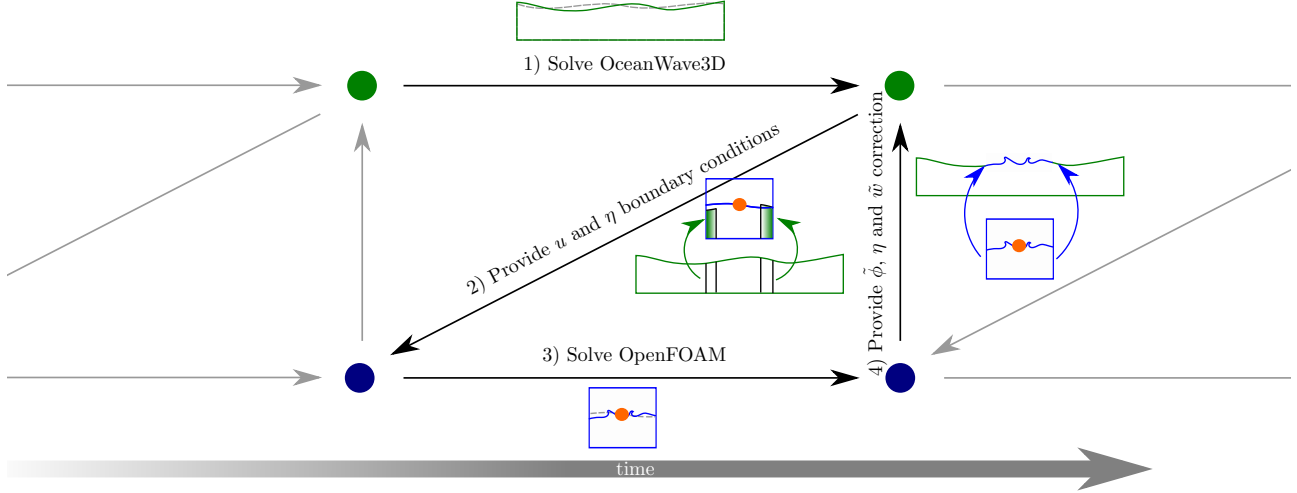


Fig. 2. Time step schematic. 1) the FNLPF problem is solved by OceanWave3D in the entire domain. 2) OceanWave3D provides boundary conditions for the RANS problem. 3) the RANS problem is solved, using the same time step size as OceanWave3D. 4) the RANS solution for the free surface quantities  $\phi$ ,  $\eta$  and  $\tilde{w}$  is imposed onto the FNLPF solution.

2 and 4. This can lead to very high CPL values for flat sea states. For OceanWave3D, a discretisation with 72 CPL and 15 cells in the vertical direction is chosen for all cases presented in this paper, based on convergence studies. The temporal discretisation is equal for both solvers in the nested model. A temporal discretisation of the order of 0.0025 times the wave period  $T$  was found to be sufficient.

#### E. Verification of the coupling from OpenFOAM to OceanWave3D

The proposed two-way coupled model is able to transfer the wave field from OpenFOAM to OceanWave3D. To verify this new coupling step, a case is set up, where waves are generated in OpenFOAM, then propagate into the OceanWave3D domain and are absorbed.

A nested case is used with no wave generation in the OceanWave3D domain. The domain setup for this case is depicted in Fig. 3. In this case, the OpenFOAM wave field is not transferred to OceanWave3D in the entire area occupied by the OpenFOAM domain, but only in the area underlined red in Fig. 3. The OceanWave3D solution is transferred to OpenFOAM in the two-way coupling zone (red filling in Fig. 3), to ensure a smooth and reflection-free propagation of the waves from the OpenFOAM to the OceanWave3D domain.

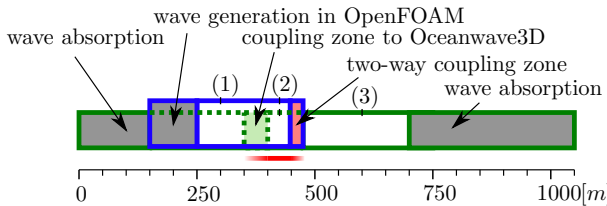


Fig. 3. Test setup for verification of the coupling from OpenFOAM to OceanWave3D, OpenFOAM domain (blue outline) and OceanWave3D domain (green outline) in side view ( $xz$ ). The area in which the OpenFOAM solution is imposed onto the OceanWave3D solution is underlined red. The numbers (1), (2)... mark the positions of numerical wave probes.

A two-dimensional discretisation of hexahedral cells was chosen for the OpenFOAM domain, with 20 CPH and 167 CPL. The mesh was refined towards the still water surface. The resulting mesh featured 70000 cells, whereas the OceanWave3D mesh featured 11880 cells. A monochromatic sea state was chosen, with  $h = 70[m]$ ,  $H = 1.5[m]$  and  $T = 8[s]$ . This represents a linear, but realistic full scale wave [24]. The case was run for a simulated time of 300[s], using a fixed time step size of  $0.0025T$ . Time signals of the surface elevation were captured at the three wave probe positions marked in Fig. 3, and the mean wave height over several consecutive wave periods was calculated by means of the phase averaging approach, described by Windt *et al.* [25]. Finally, the wave height in the OpenFOAM and OceanWave3D domain was compared to the target value, to determine the accuracy of the developed two-way coupling. As a measure for accuracy, the mean wave height error  $\epsilon$  was used.  $\epsilon$  is defined in terms of the measured and target mean wave height  $H$ , as in (13). The results in Table I show  $\epsilon$  for the different wave probe positions marked in Fig. 3.

$$\epsilon = \frac{H_{\text{measured}} - H_{\text{target}}}{H_{\text{target}}} 100\% \quad (13)$$

TABLE I  
RESULTS FOR VERIFICATION OF THE COUPLING FROM OPENFOAM TO OCEANWAVE3D, WAVE HEIGHT ERROR AT DIFFERENT PROBES

Probe	x-Pos. [m]	OpenFOAM $\epsilon$ [%]	OceanWave3D $\epsilon$ [%]
(1)	300	-1.75	-
(2)	425	-0.52	-0.29
(3)	600	-	-1.95

From Table I, it can be seen that, at probe (1), half a wave length down-wave from the wave generation zone, a wave height error of  $-1.75\%$  is present in the OpenFOAM domain. At probe (2), where the OpenFOAM solution is imposed onto the OceanWave3D solution, the error is much smaller. The relative error between OpenFOAM and OceanWave3D is very

small, as may be expected, since the OpenFOAM solution is strongly imposed onto the OceanWave3D solution here. At probe (3), which is located 1.25 wave lengths down-wave from the two-way coupling zone, a wave height error of  $-1.95\%$  is present in the OceanWave3D wave field. This error is considered relatively small for this preliminary verification of the two-way coupling approach. It is thus concluded that the implemented approach is capable of transferring waves from OpenFOAM to OceanWave3D with reasonable fidelity.

#### F. Verification of two-way wave propagation

Having verified the approach of transferring the solution from OpenFOAM to OceanWave3D, it has to be shown that a continuous wave field, of incident and reflected waves, can be developed between the OpenFOAM and OceanWave3D domains, with waves propagating in both directions at the same time. Thus, a test was set up, featuring a wave generation zone in the OceanWave3D domain (green outline in Fig. 4) and a reflective wall in the OpenFOAM domain (blue outline in Fig. 4), which is not present in the OceanWave3D domain. The results were compared to an equivalent pure OpenFOAM case, which is also depicted in Fig. 4. In the nested case, the OpenFOAM solution is imposed onto OceanWave3D in the area underlined red in the upper schematic of Fig. 4.

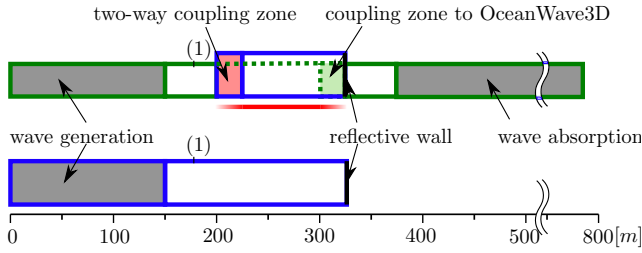


Fig. 4. Test setup for coupled case (upper schematic) and pure OpenFOAM case (lower schematic) for verification of two-way wave propagation, OpenFOAM domain (blue outline) and OceanWave3D domain (green outline) in side view ( $xz$ ). The area in which the OpenFOAM solution is imposed onto the OceanWave3D solution is underlined red. The number (1) marks the position the numerical wave probe.

Again, a two-dimensional discretisation of hexahedral cells was chosen in the OpenFOAM domain, with 20 CPH and 167 CPL. The mesh was refined 5 times in the vertical and 3 times in the horizontal direction towards the still water surface, resulting in an OpenFOAM mesh of overall 14500 cells for the coupled case and 37300 cells for the pure OpenFOAM case. The OceanWave3D mesh featured 8350 cells. The same monochromatic sea state as in Section IV-E was chosen, with  $h = 70[m]$ ,  $H = 1.5[m]$  and  $T = 8[s]$ . The cases were run for a simulated time of  $200[s]$ , using a fixed time step size of  $0.0025T$ .

Fig. 5 shows the surface elevation time traces of probe (1) (see Fig. 4). Results for the one-way coupling and for the proposed two-way coupling are presented as well as the pure OpenFOAM results.

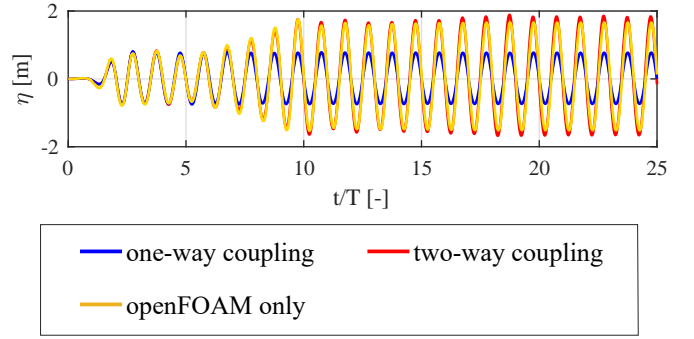


Fig. 5. Results for verification of two-way wave propagation, surface elevation over time normalised by wave period for wave probe (1)

It can be seen, from Fig. 5, that the results for the two-way coupled method are close to the pure OpenFOAM results, whereas the results for the one-way coupling are unaffected by the presence of the reflective wall in the OpenFOAM domain. This is expected, since the one-way coupling does not transfer any solution information from the RANS solver to the PF solver. Thus, the PF solver has no knowledge of the reflective wall and the corresponding reflection of the wave field in the OpenFOAM domain. From these results, it is concluded that the implemented two-way coupling approach is capable of handling waves travelling through the two-way coupling zone in both directions at the same time. A continuous wave field can thus develop between both domains.

#### G. Validation against theory

After the verification presented in Sections IV-E and IV-F, a validation study was carried out with a number of simple two-dimensional cases, considering wave propagation only. The test cases include four different monochromatic, deep water sea states, with a wave length of  $100[m]$  and increasing steepness. An overview of the sea states is given in Table II.

TABLE II  
SEA STATES FOR VALIDATION AGAINST THEORY

Sea state No.	$h[m]$	$H[m]$	$T[s]$	$h/\lambda[-]$
1	70	1.5	8.0	0.015
2	70	3.0	8.0	0.03
3	70	4.5	8.0	0.045
4	70	6.0	8.0	0.06

The domain setup is depicted in Fig. 6, following the color code of Figs. 3 and 4. The depth was  $70[m]$  in all cases and a height of  $10/3H$  above the still water level was chosen for the OpenFOAM domain, to allow for a similar discretisation and similar air flow for all sea states.

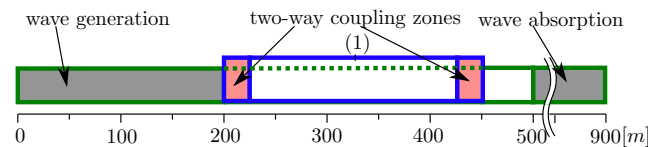


Fig. 6. Test setup for validation against theory, OpenFOAM domain (blue outline) and OceanWave3D domain (green outline) in side view ( $xz$ ). The number (1) marks the position of the numerical wave probe.



The two-dimensional spatial discretisations of hexahedral cells, with 15 CPH and a maximum cell aspect ratio of 2, featured 5 and 4 grid refinement steps towards the still water surface in the vertical and horizontal directions, respectively. The cell count for the OpenFOAM domains ranged from 16120 to 48980.

The OceanWave3D domain was discretised with 9720 cells for all sea states. The cases were run for a simulated time of  $200[s]$  with a time step size of  $0.0025T$ . Before the nested model was run, OceanWave3D ran alone for a simulated time of  $100[s]$ , to provide a fully developed sea state, as an initial condition for OpenFOAM. For all cases, the surface elevation at wave probe (1) ( $x = 325[m]$ ) was measured, the mean wave height was obtained using the phase averaging approach described in [25], and the wave height error  $\epsilon$  was calculated, following (13). The results of this study are given in Table III.

TABLE III  
RESULTS OF VALIDATION AGAINST THEORY, WAVE HEIGHT ERROR AT PROBE (1) FOR DIFFERENT SEA STATES

Sea state No.	1	2	3	4
$h/\lambda[-]$	0.015	0.03	0.045	0.06
$\epsilon$ [%]	-0.15	-0.89	-1.30	-1.58

It can be seen from Table III that the wave height error  $\epsilon$  grows with wave steepness. However, the error remains of the order of one percent of the target wave height, which is considered small [25].

#### H. Validation against experiments

A further validation study was carried out against experimental results, presented by Beji and Battjes [26], for wave propagation over a submerged bar. Based on the experimental setup, an equivalent setup for a nested, and pure, OpenFOAM domain was derived, featuring wave generation and absorption zones, instead of the physical wave maker and beach in the experiments. The numerical setups are shown in Fig. 7.

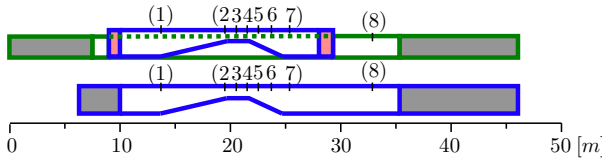


Fig. 7. Test setup for coupled case (upper schematic) and pure OpenFOAM case (lower schematic) for validation against experiments, OpenFOAM domain (blue outline) and OceanWave3D domain (green outline) in side view ( $xz$ ). The numbers (1), (2)... mark the positions of numerical wave probes.

From the different monochromatic sea states considered in [26], a single sea state with  $h = 0.4[m]$ ,  $H = 0.02[m]$  and  $T = 2[s]$  was studied here, since it avoids wave breaking over the shallow part of the domain. This flat, linear, model scale sea state built up in the experiments to a steep non-breaking wave above the shoal.

A two-dimensional discretisation of hexahedral cells was chosen for both OpenFOAM domains. A convergence study was carried out for the OpenFOAM setup. Because of the

strong morphological changes in the waves, over the length of the domain, the mean wave height could not be taken as a parameter for a convergence study and no convergence measures could be calculated. Thus, the appropriate discretisation had to be identified by visual inspection. It was concluded that a medium discretisation with 10 CPH and 924 CPL, leading to an overall cell count of 357320 for the pure OpenFOAM case, and 263530 for the nested case, was sufficient for this study. This discretisation ensures a value of at least 15 CPH for the much higher waves in the area of the shoal. The OceanWave3D case featured 13425 cells. Both, the nested and pure OpenFOAM case were run for a simulated time of  $40[s]$  with a fixed time step size of  $0.0025T$ . The time traces of six surface elevation probes were compared to the experimental results presented by Beji and Battjes [26]. The results are depicted in Fig. 8, showing the surface elevation time traces, normalised by the wave period of the incident wave.

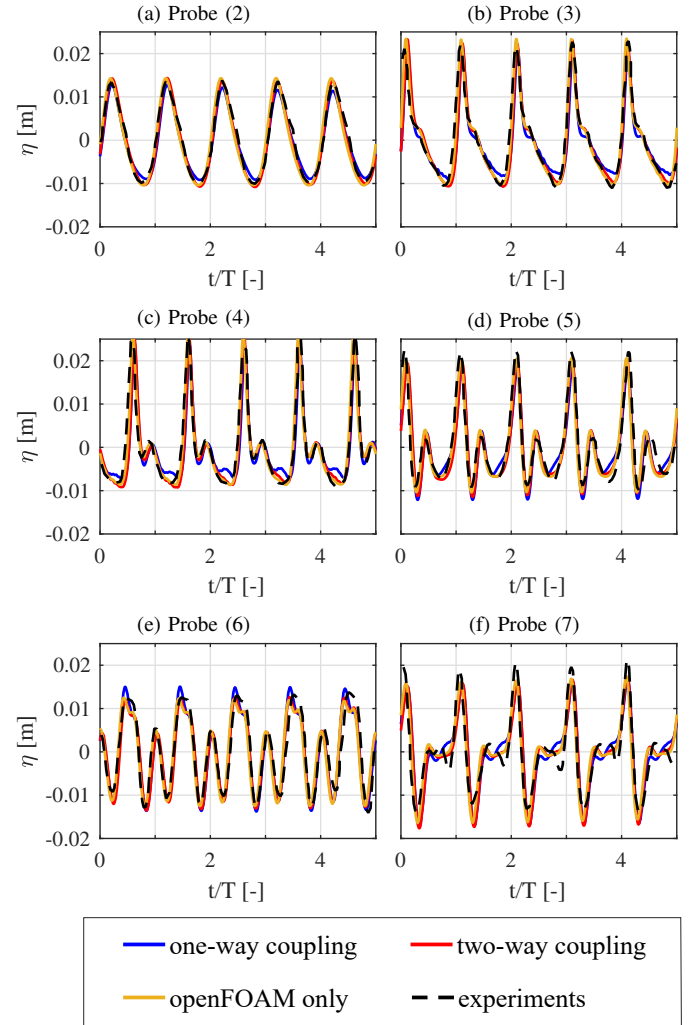


Fig. 8. Results of validation against experiments, surface elevation over time normalised by wave period

Generally, close agreement of the numerical results, compared to the experiments, can be seen for all the wave probes. Even the higher harmonics towards the end of the shoal, i.e. measurements from wave probes (4) to (7), are captured well by all the methods. However, the agreement with the

experimental results is generally better for the probes in the centre of the domain, i.e. wave probes (2) to (4). This might be due to wave reflection effects, either in the computational domain or in the experimental setup. Effects of wave reflection from the OpenFOAM outlet boundary can be observed clearly for the one-way coupling at probes (4) to (7). This is not surprising, since a strong misfit is present between the initial sea state in the OceanWave3D domain, and the obtained solution at the outlet of the OpenFOAM domain, which cannot be dampened out within the short outlet relaxation zone. Since the OceanWave3D solution is corrected with the OpenFOAM solution in the case of the two-way coupling, the reflection does not occur in that case.

A comparison of the CPU times was performed between all three cases. To allow a fair comparison, all cases were run on a single processor of a dedicated server<sup>1</sup>. Table IV shows the CPU times for the different configurations.

TABLE IV  
VALIDATION AGAINST EXPERIMENTS, CPU TIMES

Case	CPU time per simulated second [-]
pure OpenFOAM	1687
One-way Coupling	1099
Two-way Coupling	1266

From Table IV it may be concluded that, with the two-way coupled model, computational gains of 25% of the CPU time can be achieved, while maintaining a comparable accuracy with respect to the pure OpenFOAM case, and avoiding wave reflection from the OpenFOAM outlet boundary, which is present in the one-way coupled case. However, the added functionality of the two-way coupling leads to a moderately increased computational cost of 15% when compared to the one-way coupled model by Paulsen *et al.* [12].

## V. CASE STUDY

After having verified and validated the proposed two-way coupling in the previous section using simple cases, this section aims to evaluate the potential of the two-way coupling with respect to the objective of developing a two-way coupled, nested, hydrodynamic model for wave energy applications. However, since moving meshes and three dimensional cases have not been validated yet, a full study of a wave energy device was not considered appropriate. It was therefore decided to model the strong disturbance in a wave field caused by a submerged, rather than a surface piercing, structure. For this reason, the two-dimensional submerged bar case, which has already been validated in Section IV-H, is the basis of the case study, presented in the following.

To be able to evaluate the potential of the method for large scale array interaction of WECs, two submerged bars are located in two separate OpenFOAM domains which are connected through the OceanWave3D domain. An equivalent case was set up exclusively using OpenFOAM, without the nested model. A schematic of both cases is shown in Fig. 9.

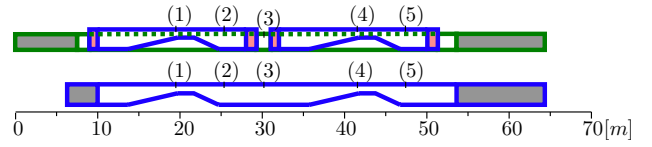


Fig. 9. Test setup for coupled case (upper schematic) and pure OpenFOAM case (lower schematic) for multi domain case study, OpenFOAM domain (blue outline) and OceanWave3D domain (green outline) in side view ( $xz$ ). The numbers (1), (2)... mark the positions of numerical wave probes.

The setup of the computational mesh used for OpenFOAM was equivalent to the one used in Section IV-H, with a discretisation of 10 CPH and 924 CPL. The mesh for the pure OpenFOAM case featured 610060 hexahedral cells, whereas the nested case was discretised with 527060 cells for the OpenFOAM domain and 18810 cells for the OceanWave3D domain. Both cases were run for 60[s] simulated time, with a fixed time step size of  $0.0025T$ . As in Section IV-H, a flat, linear, model scale sea state with  $h = 0.4[m]$ ,  $H = 0.02[m]$  and  $T = 2[s]$  was considered.

The surface elevation was evaluated at several positions in the first and second OpenFOAM domain, and between the two, in the OceanWave3D domain (see Fig. 9). At the same positions as in the nested case, the surface elevation was also probed in the pure OpenFOAM case. The time traces of the surface elevation from both cases are shown in Fig. 10.

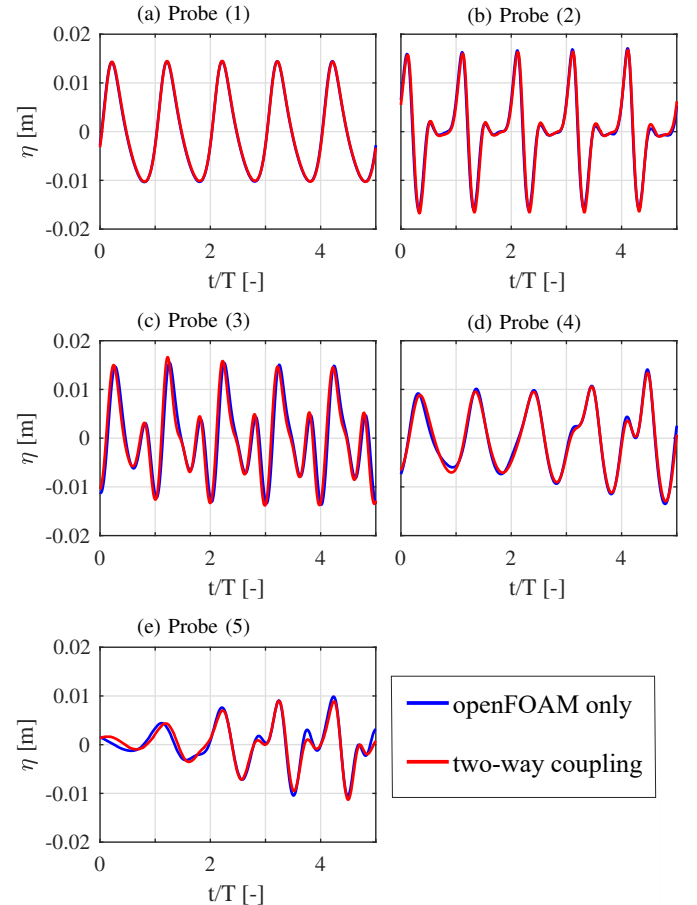


Fig. 10. Results of evaluation of a multi domain case, surface elevation over time normalised by wave period

<sup>1</sup>Dell PowerEdge with 48GB RAM and 24 Intel Xeon(R) E5-2440 processors with 2.4GHz



From the results shown in Fig. 10, some observations can be made. Generally, it can be seen that, despite the long simulated time, a steady state wave field does not develop. Due to the large distance between the submerged bars, it takes a long time for all interaction phenomena to fully develop. However, strong interaction phenomena can already be observed in the transient phase of the simulation. This becomes evident when the results for probes (1) and (2) in Fig. 10 are compared to probes (2) and (7) in Fig. 8, respectively, which show the signals of probes at the same locations with respect to the first shoal. Comparing the results for the nested model to the pure OpenFOAM results, it can be seen that all harmonics are generally captured well by the two-way coupled model. As expected from the results of Section IV-H, the results for the nested model are very close to the pure OpenFOAM results, for probes (1) and (2). Also for probe (3), a good agreement between the results for the nested and pure OpenFOAM model can be seen. However, the reflection effects towards the end of the displayed time trace show some larger differences. A small phase error can also be identified between the signals. Probes (4) and (5) confirm the earlier conclusion that all harmonics are captured well by the coupling. However, also at these locations, larger errors occur towards the end of the simulated time.

Generally it can be concluded, that the proposed two-way coupled model has the potential of capturing interaction effects between structures, placed in different OpenFOAM domains, which are connected through OceanWave3D, with an accuracy similar to a pure OpenFOAM case. It can thus be used for efficient studies of WEC array interaction effects.

## VI. LIMITATIONS

Even though the novel, two-way coupled nested model was successfully validated, and its potential for larger scale wave-structure interaction has been shown, it is still subject to some limitations, which could not be addressed within the scope of this paper. Specifically, these limitations are:

- No ability to run parallelised cases
- No ability to filter the OpenFOAM free surface signal before coupling it to a three-dimensional OceanWave3D case

To date, no efficient parallelisation of the two-way coupled method developed in this paper has been implemented. This results in the method being unsuitable for solving large RANS problems on multiple processors. This problem initially arises from the coupling methodology implemented here, which introduces some challenges regarding parallelisation. The coupling is achieved through direct integration of the OceanWave3D code into the OpenFOAM toolbox waves2Foam. Thus, OceanWave3D is executed on each of the processors used by OpenFOAM. Since OceanWave3D is not parallelised, the entire FNLPP problem is solved on each processor. This worked sufficiently well for the one-way coupling proposed by Paulsen *et al.* [12]. However, for the two-way coupling, it seems more appropriate to have OceanWave3D running on a single processor only. To achieve this, the OpenFOAM solution has to be gathered from all processors and the OceanWave3D solution has to be made available to all processors,

during the coupling procedure, which can be achieved using MPI communication.

An attempt for such a parallelisation was made in this study. However, the extensive information transfers resulted in a high demand for MPI communication, which adversely affected the computational efficiency of the method. A new approach for efficient parallelisation is thus needed. Until this new parallelisation is implemented, the method can only be run on one processor, which considerably narrows the range of application.

The second limitation was discovered when running preliminary three-dimensional simulations with the two-way coupled model. When transferring the free surface elevation and velocities from OpenFOAM to OceanWave3D, the solution always shows some scatter, due to slight inaccuracies in the VOF representation of the free surface. Thus, a Savitzky-Golay filter [27] has to be applied to the signal, before it can be written into OceanWave3D. This filter is readily implemented in OceanWave3D. However, the current implementation is only capable of filtering one-dimensional data arrays. Consequently, a sufficiently smooth solution can not be achieved for three dimensional cases, where the free surface is stored in a two dimensional array. Savitzky-Golay filters are generally capable of filtering two- and higher-dimensional arrays. Until a two-dimensional filter is implemented, the method might be prone to instability for three-dimensional simulation.

## VII. CONCLUSIONS

In the framework of this study, a novel nested hydrodynamic model, coupling the FNLPP solver OceanWave3D to the OpenFOAM wave generation and absorption toolbox waves2Foam in a two-way fashion, has been developed and implemented. The following conclusions can be drawn from this paper:

- A two-way coupled nested hydrodynamic model is best suited for efficient wave energy NWTs, since it avoids artificial wave reflection and opens up the possibility of studying large scale interaction in WEC arrays.
- The stability and accuracy of the proposed nested model was proven through verification and validation studies.
- The cases shown in this paper indicate a strong potential of the proposed nested model to significantly decrease the required CPU time for many NWT applications, even though the added functionality of the two-way coupling adds some computational cost, with respect to the one-way coupling proposed by Paulsen *et al.* [12].

## VIII. FUTURE WORK

Even though the proposed nested method showed good potential for the application in wave energy NWTs, it still suffers from some limitations, as detailed in Section VI. These limitations have to be addressed for the method to become widely applicable to wave energy problems.

An efficient parallelisation of the two-way coupling needs to be implemented. Based on the experience described in Section VI, the following objectives for this parallelisation

can be formulated. An efficient parallelisation needs to run OceanWave3D on a separate processor not involved in the OpenFOAM solution process. To achieve this, the coupling methodology needs to be changed from the implemented direct integration of the source code to a server-client architecture, where OpenFOAM and OceanWave3D can be run on separate processors. A successful implementation of this approach would not only open the possibility of handling large OpenFOAM cases but might also strongly increase the computational efficiency of the method.

The implementation of a two-dimensional Savitzky-Golay filter, which is capable of filtering the OpenFOAM surface elevation signal for three-dimensional cases before it is introduced into OceanWave3D, represents a further subject for future work. This would have a significant influence on the stability of the method for three dimensional cases.

Finally, the verification and validation should be extended towards more realistic wave energy cases, including three spatial dimensions and moving meshes.

#### ACKNOWLEDGEMENT

Jost Kemper is supported by the German Academic Scholarship Foundation. Christian Windt is supported by Science Foundation Ireland under Grant No. 13/IA/1886. The authors are grateful to the Irish Centre for High-End Computing (ICHEC) and Dr. David Malone (Maynooth University), who have provided valuable advice for the parallelisation of the proposed method.

#### REFERENCES

- [1] C. Windt, J. Davidson, and J. Ringwood, "High-fidelity numerical modelling of ocean wave energy systems: A review of computational fluid dynamics-based numerical wave tanks," *Renewable and Sustainable Energy Reviews*, vol. 93, 06 2018.
- [2] M. Penalba, G. Giorgi, and J. V. Ringwood, "Mathematical modelling of wave energy converters: a review of nonlinear approaches," *Renewable and Sustainable Energy Reviews*, vol. 78, pp. 1188–1207, 2017.
- [3] M. Penalba, J. Davidson, C. Windt, and J. V. Ringwood, "A high-fidelity wave-to-wire simulation platform for wave energy converters: Coupled numerical wave tank and power take-off models," *Applied Energy*, vol. 226, pp. 655–669, 2018.
- [4] E. Campana, A. D. Mascio, P. G. Esposito, and F. Lalli, "Viscous-inviscid coupling in free surface ship flows," *International Journal for Numerical Methods in Fluids*, vol. 21, pp. 699–722, 1995.
- [5] A. Iafrati and E. F. Campana, "A domain decomposition approach to compute wave breaking (wave-breaking flows)," *International Journal for Numerical Methods in Fluids*, vol. 41, pp. 419–445, 2003.
- [6] M. Greco, O. M. Faltinsen, and M. Landrini, "Numerical simulation of heavy water shipping," in *Proceedings of the 17th Workshop on Water Waves and Floating Bodies*, Cambridge UK, 2002, pp. 14–16.
- [7] C. Lachaume, B. Biaisser, S. T. Grilli, P. Fraunié, and S. Guignard, "Modeling of breaking and post-breaking waves on slopes by coupling of BEM and VOF methods," in *Proceedings of the 13th ISOPE Conference, Honolulu, HI, USA*, 2003, pp. 353–359.
- [8] B. Biaisser, S. T. Grilli, and P. Fraunié, "Numerical simulations of three-dimensional wave breaking by coupling of a VOF method and a boundary element method," in *Proceedings of the 13th ISOPE Conference, Honolulu, HI, USA*, 2003, pp. 340–346.
- [9] S.-H. Kim, M. Yamashiro, and A. Yoshida, "A simple two-way coupling method of BEM and VOF model for random wave calculations," *Coastal Engineering*, vol. 57, pp. 1018–1028, 2010.
- [10] T. Verbrughe, J. M. Domínguez, A. J. C. Crespo, C. Altomare, V. Stratigaki, P. Troch, and A. Kortenhaus, "Coupling methodology for smoothed particle hydrodynamics modelling of non-linear wave-structure interactions," *Coastal Engineering*, vol. 138, pp. 184–198, 2018.
- [11] A. P. Engsig-Karup, H. B. Bingham, and O. Lindberg, "An efficient flexible-order model for 3D nonlinear water waves," *Journal of Computational Physics*, vol. 228, pp. 2100–2118, 2009.
- [12] B. T. Paulsen, H. Bredmose, and H. B. Bingham, "An efficient domain decomposition strategy for wave loads on surface piercing circular cylinders," *Coastal Engineering*, vol. 86, pp. 57–76, 2014.
- [13] N. G. Jacobsen, D. R. Fuhrman, and J. Fredsøe, "A wave generation toolbox for the open-source CFD library: OpenFoam®," *International Journal for Numerical Methods in Fluids*, vol. 70, pp. 1073–1088, 2011.
- [14] C. W. Hirt and B. D. Nichols, "Volume of fluid (VOF) method for the dynamics of free boundaries," *Journal of Computational Physics*, vol. 39, pp. 201–225, 1981.
- [15] H. Rusche, "Computational fluid dynamics of dispersed two-phase flows at high phase fractions," Ph.D. dissertation, Imperial College of Science, Technology and Medicine, 2002.
- [16] E. Berberović, N. P. van Hinsberg, S. Jakirlić, I. V. Roisman, and C. Tropea, "Drop impact onto a liquid layer of finite thickness: Dynamics of the cavity evolution," *Physical Review E*, vol. 79, 2009.
- [17] R. I. Issa, "Solution of the implicitly discretised fluid flow equations by operator-splitting," *Journal of Computational Physics*, vol. 62, pp. 40–65, 1986.
- [18] K. Graf, J. Meyer, H. Renzsch, and C. Preuß, "Investigation of modern sailing yachts using a new free-surface RANSE code," in *Proceedings of the Fourth International Conference on Innovation in High Performance Sailing Yachts, Lorient, France*, 2017, pp. 67–76.
- [19] H. B. Bingham and H. Zhang, "On the accuracy of finite-difference solutions for nonlinear water waves," *Journal of Engineering Mathematics*, vol. 58, pp. 211–228, 2006.
- [20] J. Larsen and H. Dancy, "Open boundaries in short wave simulations — a new approach," *Coastal Engineering*, vol. 7, pp. 285–297, 1983.
- [21] B. T. Paulsen, "Efficient computations of wave loads on offshore structures," Ph.D. The Technical University of Denmark, 2013.
- [22] J. Roenby, H. Bredmose, and H. Jasak, *IsoAdvector: Geometric VOF on General Meshes*, 2019, pp. 281–296.
- [23] V. Vukčević, "Numerical modelling of coupled potential and viscous flow for marine applications," *FAMENA Doctoral Thesis, Zagreb*, 2016.
- [24] M. Penalba, I. Touzón, J. Lopez-Mendia, and V. Nava, "A numerical study on the hydrodynamic impact of device slenderness and array size in wave energy farms in realistic wave climates," *Ocean Engineering*, vol. 142, pp. 224–232, 2017.
- [25] C. Windt, J. Davidson, P. Schmitt, and J. V. Ringwood, "On the assessment of numerical wave makers for cfd simulations," *accepted for publication in the Journal of Marine Science and Engineering*, 2019.
- [26] S. Beji and J. A. Battjes, "Experimental investigation of wave propagation over a bar," *Coastal Engineering*, vol. 19, pp. 151–162, 1993.
- [27] A. Savitzky and M. J. E. Golay, "Smoothing and differentiation of data by simplified least squares procedures," *Analytical Chemistry*, vol. 36, pp. 1627–1639, 1964.